Equilibrium and kinetic shapes of grains in polycrystals

Wolfgang Rheinheimer, John E. Blendell and Carol A. Handwerker

Abstract

The equilibrium crystal shape is a convex shape bounded by the lowest energy interfaces. In many polycrystalline microstructures created by grain growth, the observed distribution of grain boundary planes appears to be dominated at low driving forces (after long grain growth times) by the planes present in the equilibrium crystal shape. However, at earlier stages of grain growth, it is expected that kinetic effects will play an important role in grain boundary motion and morphology. Analogous to the equilibrium crystal shape, the kinetic crystal shape of seed crystals growing from a liquid at higher supersaturations is bounded by the slowest growing orientations. This study presents an equivalent construction for grain boundaries in polycrystals and uses it to determine the kinetic crystal shape for strontium titanate as a function of temperature. Relative grain boundary mobilities for strontium titanate for the low energy crystallographic orientations from seeded polycrystal experiments are used to calculate the kinetic crystal shapes as a function of temperature and annealing atmosphere. The kinetic crystal shapes are then compared to the morphologies and orientations of the interfaces of the growing seed crystals, and to the equilibrium crystal shapes, as well.

The conclusions are that (1) the kinetic crystal shape is extremely anisotropic and displays significant transitions as a function of temperature that do not mirror changes in equilibrium crystal shape, (2) the kinetic shapes observed in the microstructures are dominated by the growing side of the interface (single crystal) and not by the dissolving side (polycrystalline matrix), and (3) faster growing orientations break up into macroscopic facets composed of slower growing orientations. The implications for grain growth underscore the applicability of crystal growth models to grain growth in polycrystals. In particular, in strontium titanate, the anisotropy of the grain boundary mobility as represented in the kinetic crystal shape is expected to be reduced from five macroscopic parameters to two (interface normal) allowing for incorporation of growth rate anisotropy in simulations of microstructure evolution at the earliest stages of grain growth, i.e. at the highest driving forces.

Keywords

Grain growth; anisotropy; grain boundary mobility; grain boundary energy; equilibrium crystal shape; kinetic crystal shape; Wulff construction; strontium titanate

1. Introduction

Research on microstructure evolution in polycrystalline ceramics has recently focused on the anisotropy of the grain boundary energy and its effect on the equilibrium shape of grains and grain boundaries [1, 2]. The distribution of grain boundary planes has been found, in most cases, to be strongly related to the anisotropy of the surface energy [3]. However, there is also one case where this relationship did not hold: in strontium titanate, the equilibrium surface energy indicates decreasing anisotropy with increasing temperatures, but the grain boundary plane distribution shows greater anisotropy with increasing temperature [4, 5]. It was argued that this discrepancy is caused by a kinetic influence on the preferred grain boundary plane orientations.

In crystal growth of a single crystal into a medium of constant supersaturation, the importance of both the equilibrium crystal shape and kinetic growth shape in the determining the shape of the crystal is well-known [6-12]. The equilibrium crystal shape (ECS) occurs for a crystal with fixed volume, i.e. as the growth rate approaches zero. At high driving forces, the shape of the crystal approaches the kinetic crystal shape (KCS) which reflects the anisotropy of the growth rate [10], with a transition between these regimes as a function of supersaturation.

The constructions for the ECS and the KCS are similar. The ECS is a convex shape bounded by the lowest energy surfaces, as represented by the Wulff construction [13, 14]. Analogously, the KCS is bounded by the slowest growing planes. This is shown schematically for a circular seed crystal, with slow growth in the [01] directions (shown blue arrow in Fig. 1a) [7]. For a growing crystal, the KCS is bound by low mobility orientations as high mobility orientations cannot form stable facets. For a shrinking crystal, the KCS is dominated by high mobility orientations as orientations with a high dissolution rate will dissolve more quickly than the others forming preferably these specific orientations (red arrow in Fig. 1b).

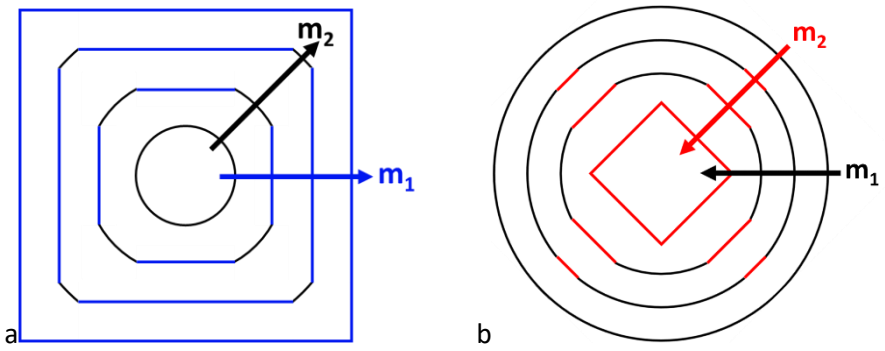

Fig. 1 Schematic of a growing kinetic crystal shape (a) and a shrinking kinetic crystal shape (b) starting from an isotropic see crystal for with $m_1 < \sqrt{2} \cdot m_2$.

In the current understanding of grain growth in polycrystalline materials, grain shapes at low driving forces (large grain sizes) are expected to be dominated by the anisotropy in the grain boundary energy, both microscopically and macroscopically [1, 3, 15, 16]. The interfacial anisotropy of a grain boundary depends on the misorientation of the two crystals and the orientation of boundary plane resulting in five macroscopic degrees of freedom [1]. The energy of a grain boundary γ_{GB} is the energy of two abutting crystal surfaces $\gamma_{s,1}$ and $\gamma_{s,2}$ minus a binding energy B:

$$\gamma_{GB} = \gamma_{s1} + \gamma_{s,2} - B \qquad 1$$

The binding energy is usually assumed to be independent of the grain boundary misorientation reducing the degrees of freedom to four. A general Wulff construction for the equilibrium "grain-within-a-grain" geometry that takes into account the resulting symmetry was reported by Blendell et al. [17]. No equivalent relationship has been established for the dependence of the kinetic grain shape on the anisotropy of grain boundary mobility.

Accordingly, this study attempts to remedy the situation by quantifying the effect of anisotropic grain boundary migration kinetics on the shape of grains during grain growth in strontium titanate polycrystals through construction of a kinetic crystal shape (KCS) and contrasting the resulting KCS with the ECS. Strontium titanate was chosen not only because of its well-established, temperature-dependent, anisotropic ECS [4, 5] but also because the anisotropy of the grain boundary mobility has

been investigated extensively [18, 19]. The previously published dataset has been supplemented here with new experimental results and used to determine the kinetic crystal shape (KCS) of strontium titanate as a function of temperature using grain growth experiments of large single crystals for four low index orientations into polycrystalline $SrTiO_3$ also undergoing grain growth.

The most important conclusions are that (1) the KCS is extremely anisotropic and displays significant transitions as a function of temperature that do not mirror changes in ECS, (2) the kinetic shapes of the migrating interfaces are dominated by the growing side of the interface (single crystal) and not by the dissolving side (polycrystalline matrix), and (3) faster growing orientations break up into macroscopic facets composed of slower growing orientations, however the resulting mobility is generally faster than required by geometry. Two consequences arise from these conclusions. First, the anisotropy of the grain boundary mobility does not need to be considered in the five-parameter space, but only with the two parameters of the growing side. Second, the crystal growth analogy for growth shapes seems to hold in polycrystals as well, although the spread in growth rates from shrinking to growing and the anisotropy of the dissolving side add considerable scatter to the shape of grains in polycrystals.

2. Experimental procedure

Most of the experimental data used in this study was published previously [4, 5, 18, 19]. Accordingly, a detailed description of the experimental procedures can be found therein. Here, the experimental procedure is briefly summarized. Both the relative mobility and the equilibrium crystal shape were measured by the seeded polycrystal technique. A single crystalline seed is diffusion-bonded to a pre-sintered polycrystalline matrix. For the polycrystalline matrix, strontium titanate powder was synthesized by the mixed oxide/carbonate method from high purity raw materials ($SrCO_3$, TiO_2, both 99.9+%, Sigma Aldrich Chemie GmbH, Taufkirchen, Germany) [20]. After pressing green bodies (cold isostatic pressing at 400MPa), samples were pre-sintered at 1425°C for 1h in oxygen in a tube furnace to a relative density of about 99%. The sintered polycrystals were sliced and polished (final step was polycrystalline diamond slurry with a particle size of 0.25µm). Subsequently, the polished surface of the polycrystals was scratched to induce pore channels during diffusion bonding. After stacking a single crystal between two polycrystalline discs, diffusion bonding was achieved during a heat treatment at 1430°C for 20min with 1MPa applied uniaxial pressure [4, 18, 19]. The stacked samples were repeatedly annealed at various temperatures between 1250°C and 1600°C in oxygen or in forming gas (5% H_2 and 95% N_2) in a tube furnace. Between the heat treatments, the microstructure was observed by scanning electron microscopy on polished cross sections.

Several different microstructural features were measured. The interface flatness of the single crystal growing into the polycrystal was characterized qualitatively relative to the original flat single crystal-polycrystal interface and its waviness relative to the grain size and shape of the polycrystalline matrix. Grain growth kinetics were assessed from measurements of the mean grain radius of the polycrystals obtained by the line intercept method. The mean growth lengths of the single crystals into the polycrystal were measured over the entire width of its interface. For the growth length, the initial position of the interface was marked by a row of small pores originating from the scratches in the polycrystal. The distance from the new position of the interface after annealing to the initial position was measured pointwise. After the longest heat treatment, the pore shapes were documented by scanning electron microscopy. In these experiments, pores at the initial position of the interface between polycrystal and single crystal were homogeneous, 1-2 µm, yielding short equilibration times of the pore shape and stable positions relative to the moving interface [4, 5, 21]. Based on multiple

images of pores, the three-dimensional shape of pores was reconstructed by fitting a calculated Wulff shape to the observed pore shape. From the calculated Wulff shape, the relative energies were obtained. For each temperature, the relative energies of approximately ten pores were averaged [4, 5].

The relative mobilities were obtained from the evolution of the growth length of the single crystals and the mean grain size of the polycrystals as a function of temperature and time. A mean field model was used to derive a suitable grain growth kinetic equation [19]:

$$L(t) = \alpha \frac{m_{sc}}{m_m}\left[3\sqrt{k_m t + 4R_0^2} - 6R_0\right] + L(t=0) \qquad \textbf{2}$$

where L(t) is the growth length of the single crystals into the polycrystalline matrix at time t, $\alpha \cong 1$ is a geometric constant, k_m refers to the grain growth coefficient of the polycrystalline matrix, and R_0 is the initial mean grain radius of the polycrystalline matrix. All these parameters are known for these experiments.

3. Results and discussion

3.1. Interfacial morphology of seeded polycrystals:

The seeded polycrystal technique was used to measure the relative mobilities of different interface orientations of strontium titanate and relate them to interface microstructure. [18, 19]. The relative mobility in Table 1 was obtained by fitting equation 2 to the growth length of the seed crystals with different crystallographic orientations [4]. According to equation 2, the growth length of the single crystals is proportional to m_{sc}/m_m, i.e. larger growth directly indicates a higher relative mobility. [18, 19]

Table 1 Relative mobility obtained by the seeded polycrystal technique. Data from the literature [18, 19] normalized to the minimum relative mobility at each temperature. Data grouped to the respective slowest orientation (i.e. {100}, {110} or {111}) at each temperature. Each group contains a calculated minimum mobility factor based on geometry as discussed in the text.

***T* [°C]**	**Relative mobility**			
	{100}	**{110}**	**{111}**	**{310}**
Cases where {100} was the slowest orientation				
1380 ox.	1.00	2.22	4.06	3.56
1550 ox.	1.00	1.54	1.90	1.32
1550 red.	1.00	2.20	1.58	2.01
1600 ox.	1.00	1.45	1.46	1.37
From geometry				
	1.00	1.41	1.73	1.05
Cases where {110} was the slowest orientation				
1350 ox.	1.22	1.00	1.92	1.52
1350 red.	1.21	1.00	1.08	1.14
1360 ox.	3.39	1.00	11.0	12.6
1400 ox.	1.39	1.00	4.69	2.01
1460 ox.	1.69	1.00	2.42	1.64
From geometry				
	1.41	1.00	1.22	1.12
Cases where {111} was the slowest orientation				
1250 ox.	2.11	1.05	1.00	1.61
From geometry				
	1.73	1.22	1.00	1.37

Figs. 2, 3 and 4 show representative microstructures for the four surface orientations of the seed crystals used in this study. A comparison shows three different microstructures observed: (1) almost flat interfaces (e.g. {110} at 1460°C in Figs. 2(b), 3(a), and 4(a)), (2) macroscopic waviness that reflects the large-scale curvature of grain boundaries between the single crystal and large grains in the polycrystalline matrix (e.g. in Fig. 2(a) and Fig. 3(d)), and (3) macroscopically facetted planes as highlighted by lines in the remaining Figs. 2-4. These macroscopic “facets” are repeating planar features along the interfaces but with local curvature due to presence of the matrix grains.

The relative mobilities measured for all temperatures and both annealing atmospheres are summarized in Table 1, with all mobilities normalized to the orientation with the minimum relative mobility at each temperature and grouped according to the lowest mobility orientation [19, 20]. At higher temperatures, the minimum mobility orientation is {100}, at intermediate temperatures, {110}, and at the lowest temperature (1250°C), {110}. The one anomaly is 1380°C, which has {100} as the slowest growth orientation. In relating the relative mobilities to the three observed interface morphologies, overall flat interfaces have low grain boundary mobilities while wavy and interfaces

with macroscopic facets have faster mobilities, regardless of the orientation of the slowest growing orientation at a given temperature. The macroscopic facets tend to form at the slowest orientations. For example, in reducing atmosphere (N_2-H_2) at 1550°C (Fig. 4), the slowest mobility orientation is {100}. For growth in the {110} and {111} directions, macroscopic facets form angles of roughly 45° to the horizontal plane in Fig. 4c and Fig. 4d corresponding to {100} planes. For growth in the {310} directions, the {100} forms at roughly 20° to the horizontal plane in Fig. 4e. It must be noted that, while these measurements are approximate, coming from 2D SEM sections of interfaces with 3D shapes, the three observed interface morphologies and their relationships to the orientations with the lowest relative interface mobility are consistent across all datasets.

For all interfaces, the grains in the polycrystalline matrix, I.e., the dissolving side of the interfaces, impose a local waviness to the shape of the interface due to local driving force being dependent on grain size. As a result, the macroscopic "facets" are not atomically flat at the scale of the grain size, but maintain a general orientation parallel to slow growing orientations in the growing single crystal. The macroscopic shape of the grain boundary is, therefore, dominated by the lattice of the growing crystal. Interestingly, these were observed whether the interface is dry (annealing in oxygen) or wetted by a liquid film (annealing in reducing atmospheres). According to the literature [18, 22], a wetting liquid phase was present at 1550°C in reducing atmosphere (Fig. 4), while all oxidizing conditions produce dry grain boundaries [19, 23-25]. For a wetted grain boundary, the grain boundary faceting can be different on the two sides as the liquid can accommodate the structural effect [17]. In contrast, for dry grain boundaries the two sides are constrained to remain in contact.

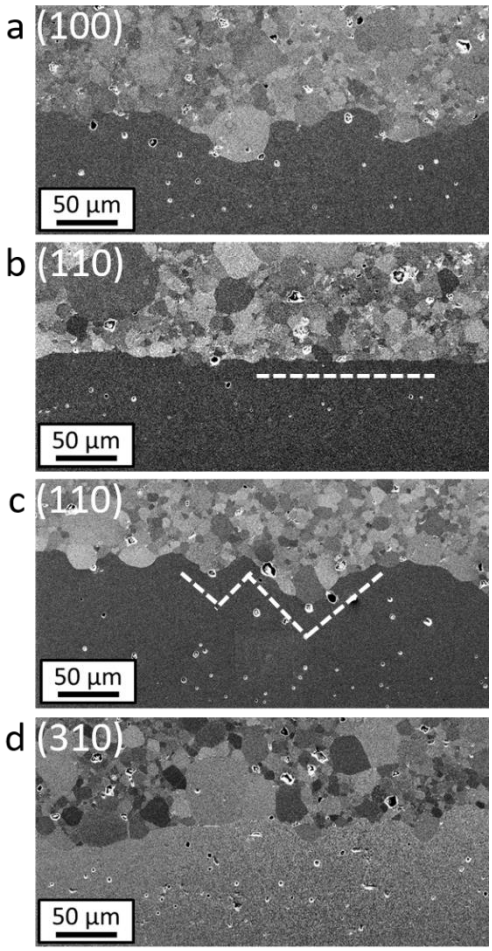

Fig 2 Morphology of the interface after 40h in oxygen at 1460°C for the orientations (a) {100}, (b) {110}, (c) {111}, and (d) {310}. In b and c, the morphology is marked by lines.

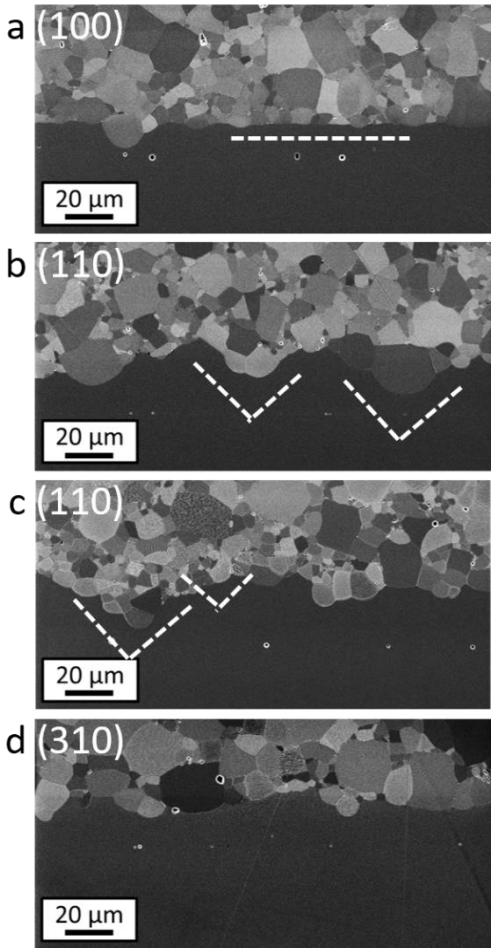

Fig. 3 Morphology of the interface after 0.1h in oxygen at 1550°C for the orientations {100} (a), {110} (b), {111} (c) and {310} (d). In a, b and c, the morphology is marked by lines.

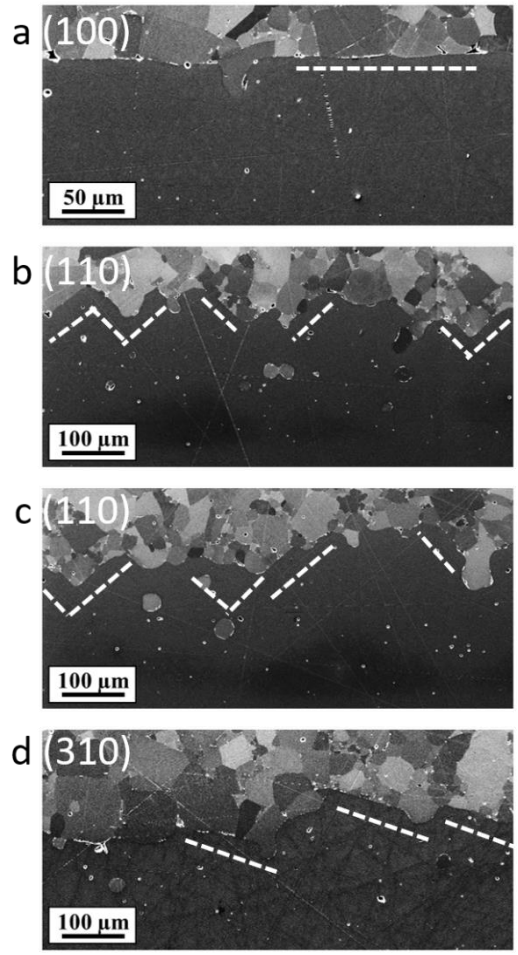

Fig. 4 Morphology of the interface after 0.4h in reducing atmosphere (N_2-H_2) at 1550°C for the orientations {100} (a), {110} (b), {111} (c) and {310} (d). In each microstructure, the morphology is marked by lines.

3.2. **Kinetic crystal shape of strontium titanate**

This observation that the shape is dominated by the growing grain sheds new light on the consideration of anisotropy of moving interfaces. The growing single crystal induces long-range structure to the interface, dominating the macroscopic shape of the interface. Given this observation, the data on the relative mobility in Table 1 from the literature [18, 19] can be used to construct the kinetic crystal shape of strontium titanate.

Fig. 5 shows the calculated kinetic crystal shapes (KCS) as a function of temperature along with the equilibrium crystal shapes (ECS) from the literature (upper row [4])[19]. The KCS for 1430°C (not shown in Fig. 5) is estimated in Appendix B and is very similar to the KCS at 1400°C and 1460°C. A comparison of the ECS and KCS for oxidizing conditions at all temperatures shows that, while the ECS generally contain {100}, {110} and {111} planes, with {310) appearing at higher temperatures, for the KCS {110} is the dominant orientation at 1460°C and lower temperatures, and {100} at higher temperatures. The dataset of 1380°C seems not to fit the trends in the other data and the reason for this behavior is not understood. However, this temperature falls into the temperature range of the well-documented grain growth transition [26-29]. The grain growth transition is characterized by the average grain growth constant of polycrystals decreasing by orders of magnitude between 1350°C and 1425°C and then increasing as temperature increases, as seen in Fig. 6. A separate discussion on this issue can be found in section 3.3.

The comparison of the ECS and KCS for reducing atmosphere is shown in Fig. 7. Again, the ECS is mostly dominated by {100} and {310}. At low temperature, the KCS mostly contains {110} planes with small {111} and {310} present as well. At 1550°C the KCS is dominated by {100}. Note that a reducing atmosphere results in a wetting second phase at the interfaces, which increases the grain growth rates significantly [18]. The KCS in reducing atmosphere (i.e. with wetting second phase at the interfaces) is almost the same as in oxidizing atmosphere (i.e. with dry interfaces).

As seen in Figs. 5 and 7, the KCS is very different from the ECS for all experimental conditions. This sheds new light on the interpretation of the published results on the grain boundary plane distributions in polycrystalline strontium titanate. In general, the grain boundary plane distribution is assumed to be correlated to the anisotropy of the grain boundary energy [1, 3]. In Fig. 5, the ECS shows decreasing anisotropy with increasing temperature with the decreasing influence of {100} with increasing temperature [4]. The expected grain boundary plane distributions based on ECS would, therefore, be expected to be dominated by {100} at low temperatures and become more isotropic at temperatures above 1460°C. In contrast, the distributions observed by Rheinheimer et al. at 1300°C, 1350°C, and 1425°C showed an increasing fraction of {100} grain boundary planes with increasing temperature. These results are consistent with Bäurer et al. [30] who showed no grain boundary planes oriented parallel to {100} at 1300°C and with Bäurer et all and Shih et all. [24, 25] who observed almost 50% were found to be oriented in {100} with respect to one of the adjacent grains at 1425°C. These measured grain boundary plane distributions are consistent with the KCS and its temperature dependence. Thus, there is experimental evidence for a kinetic impact on grain boundary plane distribution in strontium titanate and suggests that this may be important in general polycrystals undergoing grain growth. Furthermore, the grain boundary plane distribution is expected to be correlated with KCS and for individual grain boundaries, the grain boundary plane is expected to be dominated by the growing side of the grain boundary and to reach a limiting shape dictated by KCS.

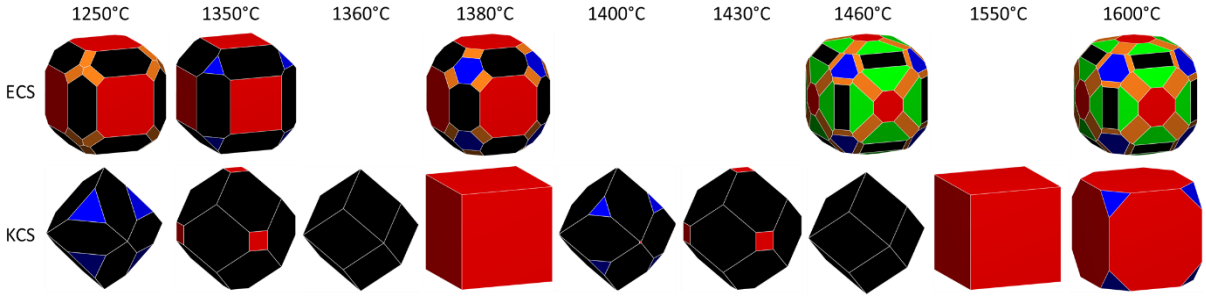

Fig. 5 Kinetic crystal shapes for oxidizing atmosphere compared with the equilibrium crystal shapes [4]. The planes are indicated as follows: {100}, red; {110}, black; {111}, blue; {301}, green; corrugated, orange. KCS at 1360°C and 1400°C constructed from previously unpublished data (provided in Appendix A). Appendix B gives an estimated KCS at 1430°C which is not significantly different from 1400°C and 1460°C.

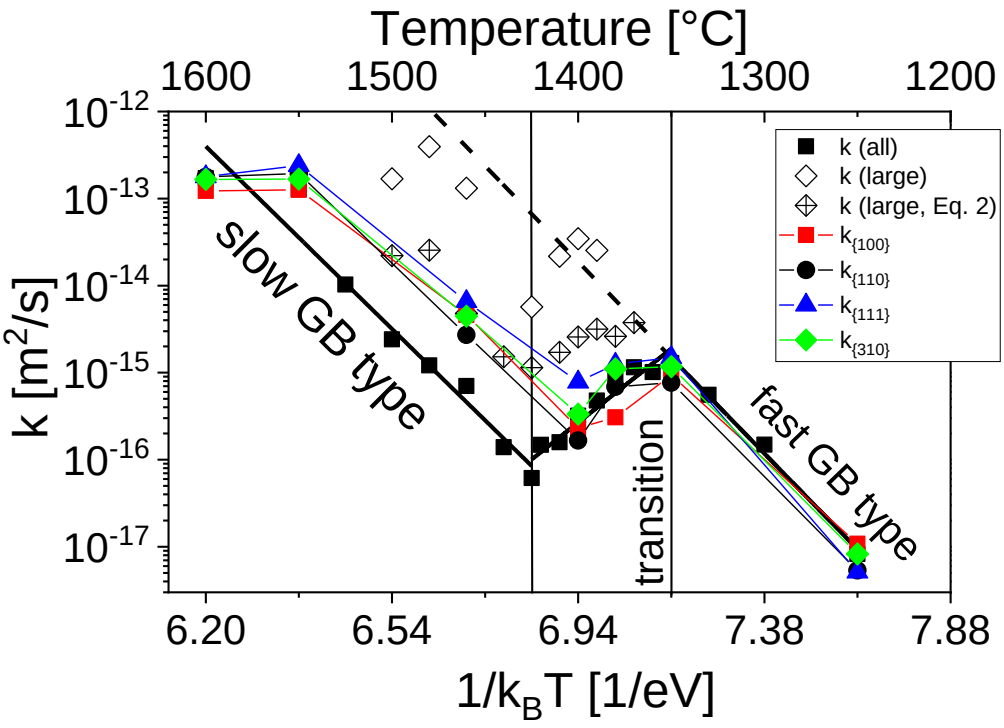

Fig. 6 Grain growth transition showing the grain growth constants of the polycrystal, of all four single crystal orientations, and abnormally growing grains in the matrix [19, 26, 29, 31]. The estimated growth rate of large grains, previously published as k (large), was re-evaluated using Eqn. 2 and shown here as k (large, Eq. 2).

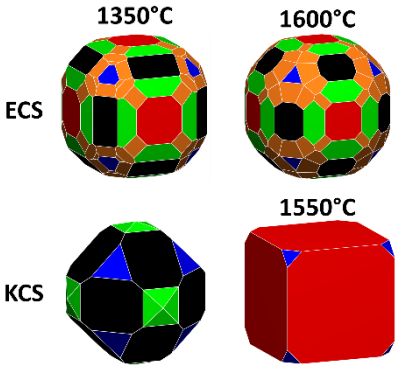

Fig. 7 Kinetic crystal shape for reducing atmosphere compared to the equilibrium crystal shape. While the anisotropy of the shapes is generally somewhat lower than for oxidizing atmosphere, the trends are the same as in oxidizing atmosphere.

3.3. Implications for the grain growth transition of strontium titanate

As noted above, strontium titanate is well-known for its grain growth transition where the grain growth rate in polycrystals first increases with increasing temperature up to 1350°C, decreases by orders of magnitude between 1350°C and 1425°C ([26-29, 31, 32], see Fig. 6), and then begins increasing again above 1425°C. In addition to the KCS, the orientation-dependent kinetic growth factors for the single crystal growth experiments are also included in Fig. 6 for comparison with the kinetic growth factors

of the polycrystalline matrix and for the abnormally growing grains in the matrix. The absolute mobilities of the single crystals as obtained by $\frac{m_{sc}}{m_m} \cdot k$ are shown in Fig. 6. The open diamonds give the growth rate of large "abnormal" grains in polycrystals as obtained by $R^2 - R_0^2 = \frac{1}{4}kt$ assuming that the large grains are surrounded by equally large grains. Using this relationship underestimates the driving force for growth if the large grains are actually surrounded by small grains, and, thus, gives an overestimation of the grain growth constant. If it is assumed that that the large grain is surrounded only by small grains, as is expected by abnormal grains before impingement, Eqn. 2 can be used to obtain a more realistic approximation for the growth constant of large grains (shown as crossed diamonds in Fig. 6). It is apparent that at 1460°C and 1550°C, the kinetic growth factors of the single crystalline seeds match well with the lower approximation of the kinetic growth factor of the large "abnormal" grains.

As shown in Fig. 6, the grain growth anomaly has been hypothesized as being due to the co-existence of two different boundary types based on mobility. A fast type was proposed to cause fast grain growth below 1350°C, while a slow type results in slow grain growth above 1425°C. From 1350°C to 1550°C, bimodal microstructures occur, suggesting that two grain boundary types coexist at higher temperatures [23-25, 29, 31, 33-37]. These regimes are annotated in Fig. 6, as proposed by Rheinheimer et al. and Kelly et al. [26, 29, 31, 32] The "fast GB type" dominates the microstructure at low temperatures due to impingement of fast-growing grains. Thus, the slow-growing grains are not present at low temperatures, having been consumed by the impinging fast-growing grains. A bimodal grain size distribution is apparent at temperatures above the transition at 1350°C, with a growing difference between the kinetic growth factors of the matrix grains and the large "abnormal" grains. This means that the bimodality becomes increasingly obvious in the transition region, with an increasing difference between the kinetic growth factors of the polycrystalline matrix and the large grains.

The observed grain boundary plane distributions were found to be consistent with KCS at both low and high temperature. This means that the orientations of "fast GB type" grain boundaries at low temperatures which had already impinged are {110} orientations, while the "slow GB type" at high temperatures, predominantly the polycrystalline matrix, are dominated by {100} orientations. Based on the extrapolation of the "slow GB types" to low temperatures, it is not known whether the polycrystalline matrix before impingement might have been dominated by {100} or the large "abnormal" grains at high temperature by {110}.

As seen Fig. 5, there are multiple transitions observed in the KCS within the transition region. At 1380°C, the KCS is dominated by {100}, although this temperature falls into the fast grain growth regime in Fig. 6 (and, thus, should be dominated by {110}). At 1460°C, the situation switches: the observed KCS is dominated by {110}, although this temperature is in the slow grain growth regime and the KCS should be dominated by {100}. This behavior may be traced back to specific orientations of the single crystalline seeds not growing with the same grain boundary type as the grains in the polycrystal. An additional complicating factor is the relative growth rates of the polycrystalline matrix and the single crystal seeds into the polycrystalline matrix. For example, at 1380°C, the {100} single crystals grow relatively slowly with a mobility of 0.36 of the mobility of the polycrystal [19]. This behavior can be understood such that the {100} single crystal transformed to the low mobility type. At least some orientations in the range of 1350°C to 1400°C fall below the kinetic growth factor for the matrix. At 1550°C and 1600°C, {100} was found to be the slowest orientation, dominating the KCS as shown in Fig. 5. The kinetic crystal shape found at 1380°C agrees well with those found at 1550°C and 1600°C. Accordingly, the data at 1380°C could represent the kinetic crystal shape of the slow grain boundary

type although the grain boundaries in the polycrystal still follows mostly the fast GB type. Finally it should be noted that, while two types of grains are present in strontium titanate, “fast GB type” and “slow GB type”, it is still not clear what makes one grain boundary a fast GB type and another a slow GB type.

3.4. Implications for our understanding of grain growth

It has been shown that, in many cases of polycrystals annealed for long time such that the grain growth rate is slow, the orientations of grain boundaries are dominated by the orientations in the ECS. In contrast, the present study shows that in a strontium titanate polycrystal undergoing grain growth, the observed orientations are those present in the KCS. It was observed that the shapes of the interfaces are dominated by the growing single crystal while the shrinking polycrystalline grains affect local curvature but not the macroscopic growth anisotropy. This suggests that the local anisotropic mobility for grain boundaries is determined by the orientation of the growing side, and can be predicted from the orientation-dependent mobilities, e.g. from experiments like those presented above. These findings suggest that concepts from crystal growth with attachment-controlled growth kinetics can be applied to solid-state grain growth in single-phase polycrystals before stagnation occurs.

A surprising result shown in Table 1 is that, for interface orientations forming inclined macroscopic facets in the slowest growth directions, their observed relative mobilities did not correspond to the net geometrical growth of two slower growing facet orientations. For example, if {100} is the slowest mobility orientation, {110} might be expected to form {100} facets with growth higher than {100} by $\sqrt{2}$ as given by the angle of 45° between {100} and {110}. The expected geometrical growth factors are $\sqrt{3} = 1.73$ for {111} and 1.05 for {310}. For {110} as the slowest mobility orientation, the corresponding growth factors for {100}, {111} and {310} are 1.41, 1.22 and 1.11, respectively. For {111} as the slowest mobility orientation, the corresponding growth factors for {100}, {110} and {310} are 1.73, 1.22 and 1.37, respectively. As seen in Table 1, these ratios are generally not observed. Most orientation have significantly higher net mobilities than expected from geometry, although the trends are followed in general as evident in Fig. 8a-c. The reason for this difference might be the atomic migration mechanism of grain boundaries compared to liquid-solid interfaces in crystal growth. In crystal growth the growing interface is not constrained by an abutting crystal. On the atomic scale, grain boundary migration occurs by the translation of atoms from the lattice of the shrinking grain to the adjacent growing one. While the specific mechanisms for grain boundary migration are not fully understood, it is known that grain boundaries migrate by the motion of disconnections [23, 34, 35, 38-40]. It is likely that disconnections and their migration kinetics are causing the differences between the observed differences between the observed orientation-dependent grain growth factors for single crystal seeds into polycrystals and the predicted geometrical growth factors based on growth of adjacent facets.

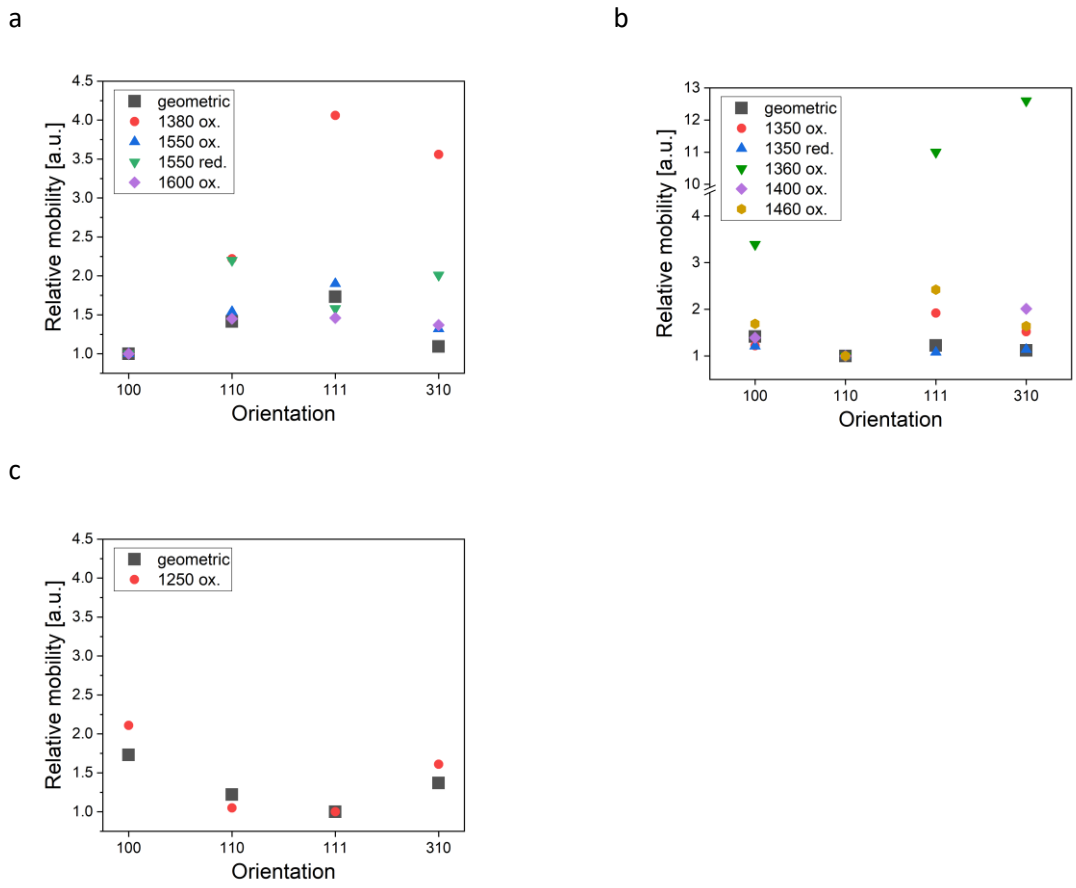

Fig. 8 Relative mobility of all datasets used in the present study along with the predictions from crystal growth theory for cases where (100) (a), (110) (b) and (111) (c) was the slowest orientation.

3.5. Comparison to previous studies

While there is considerable literature on growth rate anisotropy during crystal growth from solutions [9], relatively little information is available for the KCS during grain growth. For strontium titanate, two studies observed the growth of single crystalline seeds into a polycrystalline matrix [41, 42]. In oxidizing atmosphere and no dopant, the interfaces show very flat planes facetted in {100} or {110}. The {100} grows significantly faster than {110} at 1470°C, which agrees well with the data presented here. However, in contrast to the present experiments, the boundary plane did not break into individual macroscopic planes. Possibly this difference is related to the occurrence of sharply facetted interfaces reported in the literature [42], while curved, but macroscopically facetted interfaces are evident in Fig. 2-4 [23]. This difference in faceting is most likely related to the higher level of impurities and a wetting second phase layer observed in the cited references than in the present study [43, 44]. Another difference in the cited studies is the porosity of the polycrystal adjacent to the single crystal seeds. The seeded polycrystals were prepared from single crystals embedded in powder by SPS, so that the polycrystalline matrix close to the single crystal was not fully sintered. Accordingly, a strong impact of pore drag is expected on interface migration[45-48].

Grain growth in barium titanate has been studied in great detail [49-54]. While these studies have the same limitations regarding wetting second phases at the interfaces [49, 50] and porosity in the polycrystalline matrix [52], important findings were reported on the interfacial morphology. For facetted interfaces, {210} was found to be slower than {100} by a factor of two. While in most cases

the interfaces maintained a flat shape during growth, the {100} orientation was observed to break into {210} planes during growth for a few cases [49, 50, 52]. This behavior agrees well with the observations from this study. For alumina, several studies observed the impact of anisotropy on interfacial migration with and without the presence of a wetting second phase [55-59]. Here, the basal plane was found to remain flat during growth of the single crystalline seeds while the prismatic plane tends to have wavy interfaces [55, 56, 58, 59].

4. Summary and conclusions

This study presents a model for determining the effect of the interface mobility on grain growth in polycrystals with a specific emphasis on the grain growth anomaly in $SrTiO_3$. The interface mobility anisotropy leads to a kinetic crystal shape for grains in a polycrystalline material as an analogy to the shapes of growing crystals in a supersaturates solution during crystal growth. The KCS was constructed from mobility data for the growth of single crystalline seeds into a polycrystalline matrix as a function of growth direction of the single crystal and temperature, taking into effect the matrix grain growth on the changing driving force. The KCS and ECS were found to be very different. The ECS contains multiple facet types at all temperatures, with {100} and {110} dominating at lower temperatures. As temperature increases {301} and {111} increase in area, while {100} and {110} decrease. As reported previously (and as expected), the ECS while still being largely facetted, becomes more isotropic as temperature increases. In contrast, the KCS consists of {110} planes at lower temperatures, with only small areas of either {111} or {100} present. At higher temperatures (T≥1550°C), the KCS is dominated by {100} planes, with {111} planes present at 1600°C.

To relate the observed anisotropy of the grain boundary mobility to the local microstructure, the morphologies of the growing interfaces of single crystalline seeds in contact with polycrystalline matrix were analyzed. The slowest orientations show a relatively flat interface morphology and the higher mobilities have an unstable interface morphology: Large portions of the interface reorient to those orientations that have a low migration rate. As a result, macroscopic “facets” formed on the interface at a length scale well above the mean grain size of the polycrystal. The conclusions are that (1) the KCS is extremely anisotropic and displays significant transitions as a function of temperature that do not mirror changes in the ECS, (2) the kinetic shapes are dominated by the growing side of the interface (single crystal) and not by the dissolving side (polycrystalline matrix), and (3) faster growing orientations break up into macroscopic facets composed of slower growing orientations. The implications for grain growth underscore the applicability of crystal growth models to grain growth in polycrystals. In particular, for strontium titanate, the anisotropy of the grain boundary mobility is reduced from five macroscopic parameters to two (interface normal) allowing for more straightforward modelling of growth rate anisotropy in microstructure evolution at the early stages of grain growth, i.e. when the driving force is highest. There should then be a transition between interface shapes as the driving force for grain growth decreases. For grain boundaries that are migrating quickly the KCS is expected to play a major role in determining local interface shapes, while at lower driving forces, as the grain boundary velocities decrease, the ECS will become more important.

Overall, the present study highlights that during grain growth in anisotropic polycrystals, the anisotropy of the grain boundary mobility impacts the distribution of grain boundary planes. To approach the question which anisotropy (grain boundary energy or mobility) is more important for a given situation, the theory of crystal growth can be revisited and used as a basis to develop more advanced models for anisotropic grain growth in polycrystalline ceramics.

Acknowledgements

J.E.B. and C.A.H. thank Michael J. Hoffmann at Karlsruhe Institute of Technology in Karlsruhe, Germany for his hospitality and support during a sabbatical visit.

Appendix A

In Fig. 5, a KCS for 1360°C and 1400°C is shown that is based on the relative mobility as obtained by the seeded polycrystal technique as outlined in Section 2 and detailed elsewhere [19]. Figure S 1 shows the growth of the four different orientations for these temperatures. Fitting Eqn. 2 to the data resulted in a relative mobility of 0.601 ({100}), 0.177 ({110}), 1.947 ({111}) and 2.226 ({310}) for 1360°C. Along with a grain growth rate of the polycrystal of $1.014 \cdot 10^{-15}$ m²/s [29], the growth rates of the single crystals are $6.094 \cdot 10^{-16}$ m²/s ({100}), $1.795 \cdot 10^{-16}$ m²/s ({110}), $1.974 \cdot 10^{-15}$ m²/s ({111}) and $2.257 \cdot 10^{-15}$ m²/s ({310}). For 1400°C, the relative mobilities where 0.722 ({100}), 0.529 ({110}), 2.435 ({111}) and 1.043 ({310}). Along with a grain growth rate of the polycrystal of $3.202 \cdot 10^{-16}$ m²/s [29], the growth rates of the single crystals are $2.313 \cdot 10^{-16}$ m²/s ({100}), $1.663 \cdot 10^{-16}$ m²/s ({110}), $7.796 \cdot 10^{-16}$ m²/s ({111}) and $3.338 \cdot 10^{-16}$ m²/s ({310}).

a b

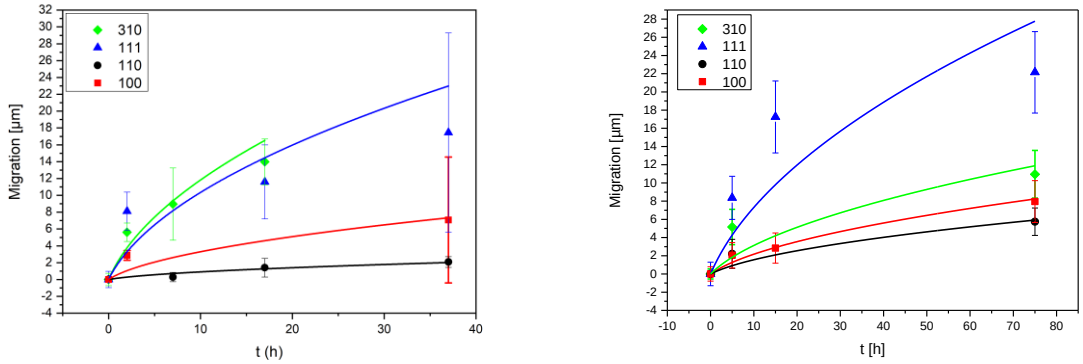

Figure S 1 Growth of single crystalline seeds into a polycrystalline matrix at 1360 (a) and 1400°C (b) in oxygen.

Appendix B

The seeded polycrystals used for the measurement of the grain boundary mobility are processed by diffusion bonding at 1430°C for 20min as detailed in the literature [4, 18, 19]. During this heat treatment, some growth of the single crystalline seeds occurred and was quantified during the procedure described in the literature. This data can be used to estimate the anisotropy of the grain boundary mobility for an additional temperature that was not considered so far. However, for this case, only one heating time is available (20mins) limiting the statistical relevance of this data. However, for each orientation, ten individual samples are available. The average growth length of these ten samples for each orientation is shown in Figure S 2. The error bars indicate the scattering among the ten samples. Assuming an initial growth length of 0, this data can be used to estimate relative mobilities for the four crystal orientations.

Applying Eqn. 2 to the data resulted in a relative mobility of 1.488 ({100}), 1.217 ({110}), 2.083 ({111}) and 1.689 ({310}). Along with a grain growth rate of the polycrystal of $1.1 \cdot 10^{-16}$ m²/s [29], the growth rates of the single crystals are $1.637 \cdot 10^{-16}$ m²/s ({100}), $1.339 \cdot 10^{-16}$ m²/s ({110}), $2.291 \cdot 10^{-16}$ m²/s ({111}) and $1.858 \cdot 10^{-16}$ m²/s ({310}). The resulting KCS is shown in Figure S 3 and agrees well with the dataset shown in Fig. 5.

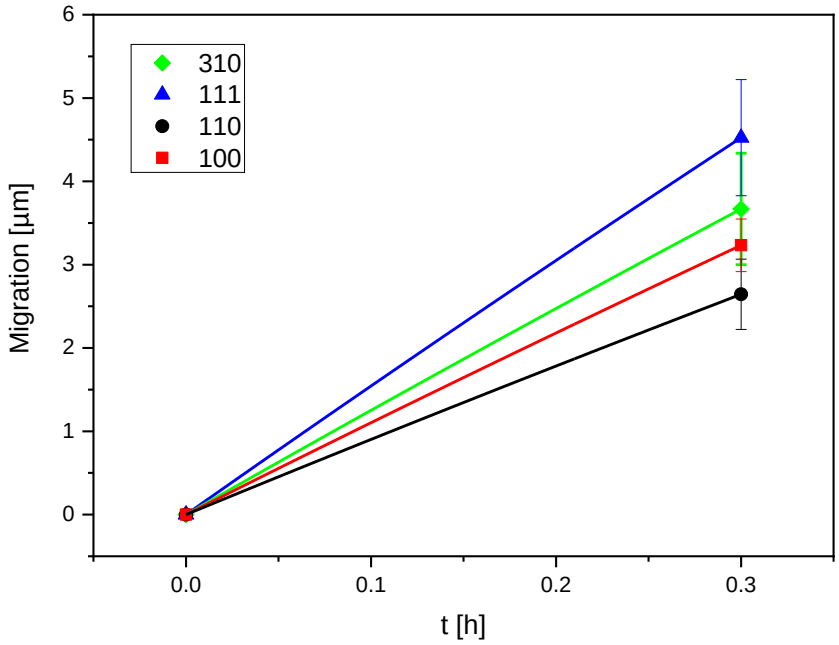

Figure S 2 Growth of single crystalline seeds into a polycrystalline matrix at 1430°C in oxygen.

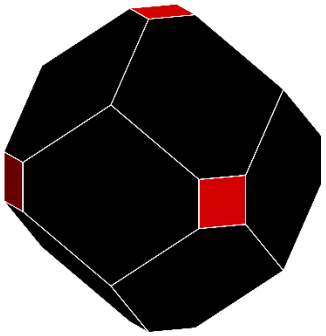

Figure S 3 Estimated KCS at 1430°C in oxygen.

References

[1] G. S. Rohrer, "Grain boundary energy anisotropy: a review," *Journal of Materials Science*, vol. 46, no. 18, pp. 5881–5895, 2011.

[2] G. S. Rohrer, "The role of grain boundary energy in grain boundary complexion transitions," *Current Opinion in Solid State and Materials Science*, vol. 20, no. 5, pp. 231 – 239, 2016. Grain boundary complexions -current status and future directions.

[3] D. M. Saylor, B. El-Dasher, Y. Pang, H. M. Miller, P. Wynblatt, A. D. Rollett, and G. S. Rohrer, "Habits of grains in dense polycrystalline solids," *Journal of the American Ceramic Society*, vol. 87, no. 4, pp. 724–726, 2004.

[4] W. Rheinheimer, M. Bäurer, H. Chien, G. S. Rohrer, C. A. Handwerker, J. E. Blendell, and M. J. Hoffmann, "The equilibrium crystal shape of strontium titanate and its relationship to the grain boundary plane distribution," *Acta Mat.*, vol. 82, pp. 32–40, 2015.

[5] W. Rheinheimer, F. J. Altermann, and M. J. Hoffmann, "The equilibrium crystal shape of strontium titanate: Impact of donor doping," *Scripta Materialia*, vol. 127, pp. 118 – 121, 2017.

[6] J. S. Wettlaufer, M. Jackson, and M. Elbaum, "A geometric model for anisotropic crystal growth," *Journal of Physics A - Mathematical and General*, vol. 27, pp. 5957–5967, SEP 7 1994.

[7] I. Sunagawa, ed., *Morphology of crystals Part A: Fundamentals*, vol. A:. Tokyo: Terra Scientific Publ., 1987.

[8] G. Müller, J.-J. Métois, and P. Rudolph, eds., *Crystal Growth - From Fundamentals to Technology*. Elsevier Science, 2004.

[9] R. F. Sekerka, "Equilibrium and growth shapes of crystals: how do they differ and why should we care?," *Crystal Research and Technology*, vol. 40, no. 4-5, pp. 291–306, 2005. 4th International Conference on Solid State Crystals/7th Polish Conference on Crystal Growth, Zakopane Koscielisko, Poland, May 16-20, 2004.

[10] W. Burton, N. Cabrera, and F. Frank, "The growth of crystals and the equilibrium structure of their surfaces," *Philosophical Transactions of the Royal Society of London Series A-Mathematical and Physical Sciences*, vol. 243, no. 866, pp. 299–358, 1951.

[11] J. Taylor, J. Cahn, and C. Handwerker, "1. geometric models of crystal growth," *Acta Metallurgica et Materialia*, vol. 40, no. 7, pp. 1443–1474, 1992.

[12] T. Uehara and R. F. Sekerka, "Phase field simulations of faceted growth for strong anisotropy of kinetic coefficient," *Journal of Crystal Growth*, vol. 254, pp. 251–261, JUN 2003.

[13] G. V. Wulff, "Zur frage der geschwindigkeit des wachstums und der auflösung der krystallflächen," *Zeitschrift für Krystallographie und Mineralogie*, vol. 34, p. 449, 1901.

[14] C. Herring, "Some theorems on the free energies of crystal surfaces," *Physical Review*, vol. 82, no. 1, pp. 87–93, 1951.

[15] G. S. Rohrer, "Influence of interface anisotropy on grain growth and coarsening," *Annual Reviews*, vol. 35, pp. 99–126, 2005.

[16] G. S. Rohrer, D. M. Saylor, B. El-Dasher, B. L. Adams, A. D. Rollett, and P. Wynblatt, "The distribution of internal interfaces in polycrystals," *Zeitschrift für Metallkunde*, vol. 95, pp. 197–214, 2004.

[17] J. E. Blendell, W. C. Carter, and C. A. Handwerker, "Faceting and wetting transitions of anisotropic interfaces and grain boundaries," *Journal of the American Ceramic Society*, vol. 82, no. 7, pp. 1889–1900, 1999.

[18] W. Rheinheimer, M. Bäurer, and M. Hoffmann, "A reversible wetting transition in strontium titanate and its influence on grain growth and the grain boundary mobility," *Acta Materialia*, vol. 101, pp. 80–89, 05 2015.
[19] W. Rheinheimer, M. Bäurer, C. Handwerker, J. Blendell, and M. Hoffmann, "Growth of single crystalline seeds into polycrystalline strontium titanate: Anisotropy of the mobility, intrinsic drag effects and kinetic shape of grain boundaries," *Acta Materialia*, vol. 95, pp. 111 – 123, 2015.
[20] M. Bäurer, H. Kungl, and M. J. Hoffmann, "Influence of Sr/Ti stoichiometry on the densification behavior of strontium titanate," *Journal of the American Ceramic Society*, vol. 92, pp. 601–606, 2009.
[21] M. Kitayama, T. Narushima, W. Carter, R. Cannon, and A. Glaeser, "The wulff shape of alumina: I. modeling the kinetics of morphological evolution," *Journal of the American Ceramic Society*, vol. 83, no. 10, pp. 2561–2571, 2000.
[22] F. Lemke, W. Rheinheimer, and M. Hoffmann, "Sintering and grain growth in $SrTiO_3$: impact of defects on kinetics," *Journal of Ceramic Society of Japan*, vol. 124, no. 4, pp. 346–353, 2016.
[23] H. Sternlicht, W. Rheinheimer, M. J. Hoffmann, and W. D. Kaplan, "The mechanism of grain boundary motion in $SrTiO_3$," *Journal of Materials Science*, vol. 51, pp. 467–475, 2015.
[24] S.-J. Shih, S. Lozano-Perez, and D. J. H. Cockayne, "Investigation of grain boundaries for abnormal grain growth in polycrystalline $SrTiO_3$," *Journal of Materials Research*, vol. 25, no. 2, pp. 260–265, 2010.
[25] M. Bäurer, S.-J. Shih, C. Bishop, M. P. Harmer, D. Cockayne, and M. J. Hoffmann, "Abnormal grain growth in undoped strontium and barium titanate," *Acta Materialia*, vol. 58, pp. 290–300, 2010.
[26] W. Rheinheimer and M. J. Hoffmann, "Non-arrhenius behavior of grain growth in strontium titanate: New evidence for a structural transition of grain boundaries," *Scripta Materialia*, vol. 101, pp. 68–71, May 2015.
[27] W. Rheinheimer and M. Hoffmann, "Grain growth transitions of perovskite ceramics and their relationship to abnormal grain growth and bimodal microstructures," *Journal of Materials Science*, vol. HTC 2015, pp. 1–10, 2015.
[28] M. Bäurer, D. Weygand, P. Gumbsch, and M. J. Hoffmann, "Grain growth anomaly in strontium titanate," *Scripta Materialia*, vol. 61, no. 6, p. 584–587, 2009.
[29] W. Rheinheimer and M. J. Hoffmann, "Grain growth in perovskites: What is the impact of boundary transitions?," *Current Opinion in Solid State and Materials Science*, vol. 20, no. 5, pp. 286 – 298, 2016.
[30] M. Bäurer, H. Störmer, D. Gerthsen, and M. J. Hoffmann, "Linking grain boundaries and grain growth in ceramics," *Advanced Engineering Materials*, vol. 12, no. 12, p. 1230, 2010.
[31] W. Rheinheimer, E. Schoof, M. Selzer, B. Nestler, and M. J. Hoffmann, "Non-arrhenius grain growth in strontium titanate: Quantification of bimodal grain growth," *Acta Materialia*, vol. 174, pp. 105 – 115, 2019.
[32] M. N. Kelly, W. Rheinheimer, M. J. Hoffmann, and G. S. Rohrer, "Anti-thermal grain growth in srtio3: Coupled reduction of the grain boundary energy and grain growth rate constant," *Acta Materialia*, vol. 149, pp. 11–18, 2018.
[33] W. Rheinheimer, M. Fülling, and M. J. Hoffmann, "Grain growth in weak electric fields in strontium titanate: Grain growth acceleration by defect redistribution," *Journal of the European Ceramic Society*, vol. 36, no. 11, pp. 2773 – 2780, 2016.
[34] H. Sternlicht, W. Rheinheimer, R. E. Dunin-Borkowski, M. J. Hoffmann, and W. D. Kaplan, "Characterization of grain boundary disconnections in $SrTiO_3$part i: the dislocation component of grain boundary disconnections," *Journal of Materials Science*, vol. 54, pp. 3694–3709, Mar 2019.

[35] H. Sternlicht, W. Rheinheimer, J. Kim, E. Liberti, A. I. Kirkland, M. J. Hoffmann, and W. D. Kaplan, "Characterization of grain boundary disconnections in $SrTiO_3$part ii: the influence of superimposed disconnections on image analysis," *Journal of Materials Science*, vol. 54, pp. 3710–3725, Mar 2019.

[36] W. Rheinheimer, X. L. Phuah, H. Wang, F. Lemke, M. J. Hoffmann, and H. Wang, "The role of point defects and defect gradients in flash sintering of perovskite oxides," *Acta Materialia*, vol. 165, pp. 398 – 408, 2019.

[37] W. Rheinheimer, J. P. Parras, J.-H. Preusker, R. A. D. Souza, and M. J. Hoffmann, "Grain growth in strontium titanate in electric fields: the impact of space charge on the grain boundary mobility," *Journal of the American Ceramic Society*, vol. 102, p. 3779– 3790, 2019.

[38] W. Rheinheimer, D. Lowing, and J. E. Blendell, "Grain growth in NiO-MgO and its dependence on faceting and the equilibrium crystal shape," *Scripta Materialia*, vol. 178, pp. 236 – 239, 2020.

[39] J. Hirth and R. Pond, "Steps, dislocations and disconnections as interface defects relating to structure and phase transformations," *Acta Materialia*, vol. 44, no. 12, pp. 4749–4763, 1996.

[40] J. Han, S. L. Thomas, and D. J. Srolovitz, "Grain-boundary kinetics: A unified approach," *Progress in Materials Science*, vol. 98, pp. 386 – 476, 2018.

[41] S.-Y. Chung, D. Y. Yoon, and S.-J. L. Kang, "Effects of donor concentration and oxygen partial pressure on interface morphology and grain growth behavior in $SrTiO_3$," *Acta Materialia*, vol. 50, pp. 3361–3371, 2002.

[42] S.-Y. Chung and S.-J. Kang, "Intergranular amorphous films and dislocations-promoted grain growth in $SrTiO_3$," *Acta Materialia*, vol. 51, pp. 2345–2354, 2003.

[43] S.-Y. Chung and S.-J. L. Kang, "Effect of sintering atmosphere on grain boundary segregation and grain growth in niobium-doped $SrTiO_3$," *Journal of the American Ceramic Society*, vol. 85, no. 11, pp. 2805–2810, 2002.

[44] S.-J. L. Kang, S.-Y. Chung, and J. Nowotny, "Effect of lattice defects on interface morphology and grain growth in $SrTiO_3$," *Key Engineering Materials*, vol. 253, pp. 63–72, 2003.

[45] J. Hötzer, M. Seiz, M. Kellner, W. Rheinheimer, and B. Nestler, "Phase-field simulation of solid state sintering," *Acta Materialia*, vol. 164, pp. 184 – 195, 2019.

[46] V. Rehn, J. Hötzer, M. Kellner, M. Seiz, C. Serr, W. Rheinheimer, M. J. Hoffmann, and B. Nestler, "The impact of pores on microstructure evolution: A phase-field study of pore-grain boundary interaction," in *High Performance Computing in Science and Engineering ' 17* (W. E. Nagel, D. H. Kröner, and M. M. Resch, eds.), (Cham), pp. 485–502, Springer International Publishing, 2018.

[47] J. Hötzer, V. Rehn, W. Rheinheimer, M. Hoffmann, and B. Nestler, "Phase-field study of pore-grain boundary interaction," *Journal of the Ceramic Society of Japan*, vol. 124, no. 4, pp. 329–339, 2016.

[48] V. Rehn, J. Hötzer, W. Rheinheimer, M. Seiz, C. Serr, and B. Nestler, "Phase-field study of grain growth in porous polycrystals," *Acta Materialia*, vol. 174, pp. 439 – 449, 2019.

[49] S.-Y. Choi, D. Yoon, and S.-J. Kang, "Kinetic formation and thickening of intergranular amorphous films at grain boundaries in barium titanate," *Acta Materialia*, vol. 52, pp. 3721–3726, JUL 12 2004.

[50] B.-K. Yoon, S.-Y. Choi, T. Yamamoto, Y. Ikuhara, and S.-J. L. Kang, "Grain boundary mobility and grain growth behavior in polycrystals with faceted wet and dry boundaries," *Acta Materialia*, vol. 57, no. 7, pp. 2128–2135, 2009.

[51] J. G. Fisher and S.-J. L. Kang, "Nonlinear migration of faceted boundaries and nonstationary grain growth in ceramics," *Materials Science Forum*, vol. 715-716, pp. 719–724, 2012.

[52] M.-G. Lee, S.-M. An, S.-H. Jung, and S.-J. L. Kang, “Migration enhancement of faceted boundaries by dislocation,” *Journal of Asian Ceramic Societies*, vol. 1, no. 1, p. 95–101, 2013.
[53] S.-Y. Choi, S.-J. Kang, S.-Y. Chung, T. Yamamoto, and Y. Ikuhara, “Change in cation nonstoichiometry at interfaces during crystal growth in polycrystalline batio3,” *Applied Physics Letters*, vol. 88, no. 1, 2006.
[54] S.-M. An, B.-K. Yoon, S.-Y. Chung, and S.-J. L. Kang, “Nonlinear driving force–velocity relationship for the migration of faceted boundaries,” *Acta Materialia*, vol. 60, p. 4531–4539, 06 2012.
[55] C. W. Park, D. Y. Yoon, J. E. Blendell, and C. A. Handwerker, “Singular grain boundaries in alumina and their roughening transition,” *Journal of the American Ceramic Society*, vol. 86, no. 4, pp. 603–611, 2003.
[56] W. A. Kaysser, M. Sprissler, C. A. Handwerker, and J. E. Blendell, “Effect of a liquid-phase on the morphology of grain-growth in alumina,” *Journal of the American Ceramic Society*, vol. 70, no. 5, pp. 339–343, 1987.
[57] B. Hockey, S. Wiederhorn, J. Blendell, J. Lee, and M. Kang, “Structure of sapphire bicrystal boundaries produced by liquid-phase sintering,” *Journal of the American Ceramic Society*, vol. 86, pp. 612–622, APR 2003.
[58] Y. Finkelstein, S. M. Wiederhorn, B. J. Hockey, C. A. Handwerker, and J. E. Blendell, “Migration of saphire interfaces into vitreous bonded aluminium-oxide,” in *Sintering of Advanced Ceramics* (C. Handwerker, J. Blendell, and W. Kaysser, eds.), vol. 7 of *Ceramic Transactions*, pp. 258–279, American Ceramic Society, 1990.
[59] J. Rödel and A. M. Glaeser, “Anisotropy of grain-growth in alumina,” *Journal of the American Ceramic Society*, vol. 73, no. 11, pp. 3292–3301, 1990.